

# Epoxy-Based Catalyst-Free Self-Healing Elastomers at Room Temperature Employing Aromatic Disulfide and Hydrogen Bonds

Geonwoo Kim, Cigdem Caglayan, and Gun Jin Yun\*

Cite This: *ACS Omega* 2022, 7, 44750–44761

Read Online

ACCESS |



Metrics &amp; More

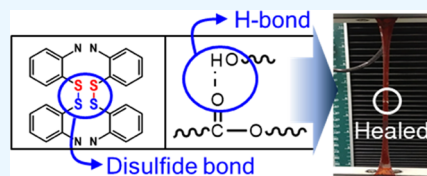


Article Recommendations



Supporting Information

**ABSTRACT:** In this paper, catalyst-free room-temperature healing epoxy vitrimer-like materials (S-vitrimer) are introduced. The S-vitrimer can be healed at room temperature without any external stimuli such as solvent, pressure, heat, and catalyst through an aromatic disulfide exchange reaction and a hydrogen bond because the glass transition temperature of the S-vitrimer is lower than room temperature. Self-healing materials are attracting widespread attention nowadays with their potential to increase the durability of the materials. However, there is still elevating need for research, considering the limitations of various self-healing methods. To the best of our knowledge, epoxy-based catalyst-free room-temperature healing materials have not been investigated until now, yet they are promising to make self-healing easier. Moreover, the S-vitrimer showed higher healing efficiency when healed for a longer time and at a higher temperature. Especially when healed at room temperature for 96 h, the S-vitrimer presented an 80% healing efficiency. The S-vitrimer also showed an 80% healing efficiency when healed at 60 °C for 48 h. To investigate the factors affecting self-healing behavior, three control experiments were carried out. Control experiments showed that the S-vitrimer is healed mainly due to a disulfide exchange reaction, but hydrogen bonds also contribute to self-healing behavior. Also, it was found that tightly packed segments can hinder self-healing through control experiments.



## 1. INTRODUCTION

Living organisms can be healed autonomously after being wounded, and they can recover their functions even if damaged. Inspired by nature, many researchers attempt to devise such a property in industrial materials to increase the durability and safety of the component. Self-healing materials are attracting enormous attention nowadays, including various industries such as aerospace,<sup>1,2</sup> automobile,<sup>3,4</sup> electronics,<sup>5–7</sup> and robotics.<sup>8–10</sup>

Many self-healing materials are fabricated employing reversible covalent bonds since they promise self-healing multiple times in the same area, avoiding additional chemicals such as healing agents or capsules. The Diels–Alder reaction,<sup>11,12</sup> boronic ester formation,<sup>13,14</sup> disulfide exchange reaction,<sup>15–18</sup> imine reaction,<sup>19,20</sup> urea exchange reaction,<sup>21,22</sup> and transesterification<sup>23–25</sup> are the reversible covalent bonds preferred to synthesize self-healing materials mostly. However, in most cases, self-healing requires external stimuli such as light,<sup>5,25–27</sup> solvent,<sup>28,29</sup> heat,<sup>23,30–33</sup> or a catalyst.<sup>34,35</sup> In such cases, the self-healing polymers cannot respond immediately under fracture because the healing mechanism needs to be triggered by external stimuli. Similarly, the incorporation of a catalyst may cause shortcomings in many ways, including but not limited to aging, stability, and toxicity.

In this scenario, the state-of-art is heading toward new industry-friendly concepts to overcome the difficulties of applying external stimuli each time. Even though a few papers reported self-healable polymers at room temperatures without external stimuli or catalysts via a disulfide bond, these self-

healable polymers mainly focused on thermoplastics and other amorphous polymers such as thermoplastic polyurethane (TPU).<sup>17,18</sup> However, TPUs are not preferred in structural components due to limitations in their utility at high temperatures. In other words, TPUs cannot be used in the aerospace industry where resistance to high temperature and high structural performance are required.<sup>36</sup> On the other hand, epoxy having a network structure possesses high heat resistance, which motivates its utility in tires and seals such as packing and gaskets in aircraft or spacecraft.<sup>37</sup> Moreover, epoxy is more facile to fabricate than TPU and more ecofriendly due to the solvent-free and catalyst-free synthesis process.<sup>38</sup> Even though there were a few studies about epoxy materials healable within reversible covalent bonds,<sup>34,39–41</sup> these research studies addressed healing with a stimulus as mentioned above, which required an additional effort. Zou et al.<sup>39</sup> studied self-healing epoxy coatings based on Diels–Alder reactions, including MXene flakes that can be activated by near-infrared (NIR) light. They observed that having MXene content allowed the epoxy to convert NIR light energy to heat quickly, enabling self-healing for nearly around 15 min.

Received: July 19, 2022

Accepted: October 20, 2022

Published: December 2, 2022



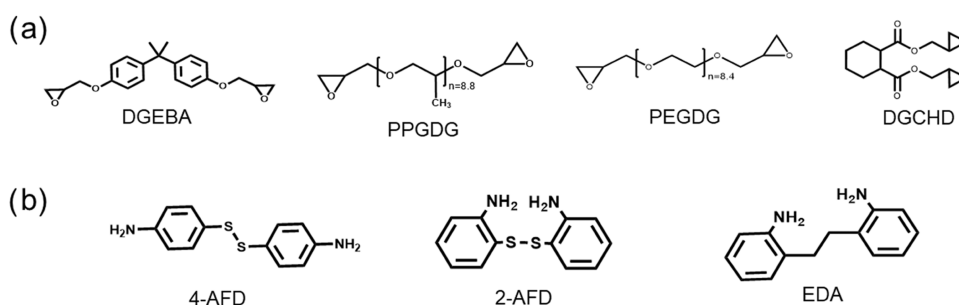


**Figure 1.** Structural formula of starting materials corresponding to (a) epoxy resin and (b) diamine.

However, in such concepts, a specific wavelength of light and high contents of flakes, capsules, powders, etc., to absorb light efficiently might be required, affecting the mechanical properties of the composite. Moreover, a self-healing mechanism based on Diels–Alder reactions might lead to a sudden viscosity drop, risking the dimensional integrity. In the case of self-healing by reversible associative covalent bonds, Capelot et al.<sup>41</sup> developed a self-healing epoxy vitrimer capable of recovering nearly 77% of its original strength at 150 °C in the presence of transesterification catalysts, though embedding catalysts in the system might result in toxicity and also induce catalyst instability. Krishnakumar et al.<sup>40</sup> stated that healing epoxy for nearly 90% of the original strength was possible by disulfide bonds, which require a heating process of the crack region to activate the bond exchange mechanism. The glass transition temperatures were around 60 °C, which prohibited the activation of disulfide exchange up to that temperature. Li et al.<sup>42</sup> also developed healing epoxy materials, but they also needed heat to repair them. Moreover, it is quite difficult to recover polymers by heating due to their low thermal conductivity. To eliminate such limitations and extra steps, this paper proposes a new approach promising good long-term structural stability and ease of repair. To the best of our knowledge, catalyst-free epoxy-based healing materials healable at room temperatures without any stimuli have not been reported yet.

Meanwhile, research works have been focused on self-healing materials, especially on vitrimers as representative polymers, which can heal intrinsically by covalently adaptable networks in the molecular structure. In other words, vitrimers own a network with exchangeable bonds so that the materials can be healed through the exchange reaction after damage. Another prominent property of the vitrimer is the decrease in its viscosity as the temperature increases, obeying the Arrhenius law. A material can be called a vitrimer when the aforementioned properties are satisfied. Materials meeting only one of these requirements are classified as vitrimer-like materials,<sup>43</sup> and this study developed vitrimer-like self-healing materials with the disulfide bond in this respect. Among the vitrimer or vitrimer-like materials, many researchers have tried to develop self-healing vitrimers with the disulfide bond,<sup>44–60</sup> which is because the disulfide bond reaction is facile to fabricate and promises high self-healing efficiency. Most of the self-healing materials with disulfide bonds, however, require external stimuli such as light,<sup>44–49</sup> heat,<sup>50–55</sup> catalyst,<sup>56–58</sup> pH,<sup>59</sup> and pressure.<sup>60</sup>

As mentioned earlier, dynamic sulfur chemistries are highly adopted in self-healing polymers, including but not limited to thiolate/nanoparticle exchange, aromatic disulfide exchange, and gold(I)–thiolate/disulfide exchange reaction.<sup>61</sup> Among

them, an aromatic disulfide bond has been preferred widely to develop room-temperature healable materials by a disulfide exchange reaction, which can take place at room temperatures.<sup>17,18</sup> Apart from that, a hydrogen bond has also been used as a self-healing agent to introduce the healing capability to the material. Many studies show that hydrogen bonds can initiate self-healing because of their reversible bond characteristics.<sup>6,17,62</sup> Specifically, Rekondu et al. developed self-healing materials with disulfide and hydrogen bonds, but it is worth noting that these materials are fabricated with TPU.<sup>17</sup> As mentioned earlier, TPUs are not ecofriendly due to the utility of solvents, and they require a complicated synthesis process. Therefore, this paper differs from the literature as the aim is to synthesize epoxy-based materials healable at room temperature without any external stimuli via disulfide and hydrogen bonds. These self-healing materials do not cause chemical waste generated from the solvent and the catalyst, implying their facile process.

Herein, to develop epoxy-based materials healable at room temperature without external stimuli, diglycidyl 1,2-cyclohexanedicarboxylate (DGCHD) was added to employ a hydrogen bond with a carbonyl group of ester. This hydrogen bond made the elastomer self-healed efficiently, as proven by Fourier transform infrared spectroscopy (FTIR) and a control experiment. Poly(propylene glycol) diglycidyl ether (PPGDG), referred to as a soft segment, was added to epoxy resin to activate the disulfide exchange reaction by decreasing the glass transition temperature ( $T_g$ ). The reason why low  $T_g$  is required is mainly that the disulfide exchange reaction occurs at temperatures lower than  $T_g$ , wherein decreasing the  $T_g$  below room temperature results in self-healing materials with elastomeric properties. The soft segments were reported before as they promote a higher healing performance, especially with the dense network, four-branched network.<sup>63</sup> Meanwhile, another study on thermoplastic polyurethane (TPU) showed that crystallinity and tightly packed segments affect self-healing behavior because the hard segment of TPU limits the segmental motion and self-healing performance.<sup>18</sup> According to the TPU study, in this research, PPGDG was used to avoid crystallinity instead of poly(ethylene glycol) diglycidyl ether (PEGDG), and 2-aminophenyl disulfide (2-AFD) was introduced due to a loosely packed segment instead of 4-aminophenyl disulfide (4-AFD). Control experiments were conducted to explore the effect of crystallinity and the tightly packed segment in epoxy.

This paper conducted synthesis, characterization, self-healing test, and control experiments of the S-vitrimer. First, the S-vitrimer self-healed at room temperature was synthesized and characterized with FTIR, thermogravimetric analysis (TGA), and differential scanning calorimetry (DSC). Then, a

tensile test was conducted to measure the healing efficiency at varying times and temperatures. The S-vitrimer showed improved self-healing performance as the healing time and temperature increased. Herein, it should be noted that self-healing occurs at room temperatures without additional external heating since the glass transition temperature ( $T_g$ ) of the produced epoxy vitrimer-like materials is lower than the room temperature. Finally, control experiments were carried out to investigate factors influencing self-healing behavior. It can be concluded that the disulfide and hydrogen bonds promoted self-healing, while the self-healing behavior was hindered by the crystallinity of the soft segment and tightly packed segments in the epoxy vitrimer-like materials.

## 2. EXPERIMENTAL SECTION

**2.1. Materials.** Bisphenol A diglycidyl ether (DGEBA), poly(ethylene glycol) diglycidyl ether (PEGDG), poly(propylene glycol) diglycidyl ether (PPGDG), diglycidyl 1,2-cyclohexanedicarboxylate (DGCHD), and 4-aminophenyl disulfide (4-AFD) were supplied from Sigma-Aldrich. 2-Aminophenyl disulfide (2-AFD) and 2,2'-ethylenedianiline (EDA) were supplied from Aladdin. All chemical reagents were used as received. Chemical structures are depicted in Figure 1.

**2.2. Synthesis of Self-Healing Epoxy Vitrimer-Like Materials.** First, the S-vitrimer was synthesized as follows. DGEBA (1 g, 2.9 mmol), PPGDG (3.76 g, 5.8 mmol), DGCHD (0.84 g, 2.9 mmol), and 2-AFD (1.94 g, 7.8 mmol) were mixed at 100 °C for 20 min by a magnetic stirrer and then degassed at 80 °C for 3 h. The resulting homogeneous liquid was poured into a silicone mold and cured at 150 °C for 15 h in an oven. Herein, the S-vitrimer was reacted with a nonstoichiometric ratio to improve the self-healing efficiency. The synthesis route is described in Scheme S1. Next, an E-vitrimer is also synthesized as follows. DGEBA (1 g, 2.9 mmol) and 2-AFD (0.36 g, 1.45 mmol) were mixed, and the rest of the process was conducted identically to the synthesis of the S-vitrimer. The synthesis route is described in Scheme S2. The P-vitrimer was prepared by the following method. PPGDG (1 g, 1.6 mmol) and 2-AFD (0.19 g, 0.8 mmol) were mixed, and the rest of the process was conducted identically to the synthesis of the S-vitrimer. The synthesis route is described in Scheme S3. The H-vitrimer is synthesized as follows. DGCHD (1 g, 3.5 mmol) and 2-AFD (0.45 g, 1.75 mmol) were mixed, and the rest of the process was conducted identically to the synthesis of the S-vitrimer. The synthesis route is described in Scheme S4. The E-, P-, and H-vitrimers were synthesized to explore why the epoxide ring of the S-vitrimer remained. Therefore, only one kind of epoxy was used in the E-vitrimer, P-vitrimer, and H-vitrimer, which is different from the S-vitrimer that included DGEBA, PPGDG, and DGCHD altogether. The E-, P-, and H-vitrimers were mixed with a stoichiometry ratio to point out the disappearance of the epoxide group peak clearly in FTIR. The control group 1 (C1) was synthesized as the following method. DGEBA (1 g, 2.9 mmol), PPGDG (3.76 g, 5.8 mmol), DGCHD (0.84 g, 2.9 mmol), and EDA (1.66 g, 7.8 mmol) were mixed, and the other process was conducted identically to the synthesis of the S-vitrimer. The synthesis route is described in Scheme S5. The only difference in C1 from the S-vitrimer was that EDA was used instead of 2-AFD as a hardener. The aim of C1 was to check the relation of self-healing with hydrogen bonds and the presence of the disulfide bond. In other words, since C1 does not have any disulfide bond, it is expected to observe the

overall effect of the hydrogen bond on the healing performance. The molar ratio of resin to the hardener is identical to that of the S-vitrimer. Control group 2 (C2) was prepared by the following method. DGEBA (1 g, 2.9 mmol), PEGDG (2.94 g, 5.8 mmol), DGCHD (0.84 g, 2.9 mmol), and 2-AFD (1.94 g, 7.8 mmol) were mixed, and the other process was conducted identically to the synthesis of the S-vitrimer. The synthesis route is described in Scheme S6. Since C2 was conducted to check the pendant group effect of the resin, only PPGDG in the S-vitrimer is replaced with PEGDG. The molar ratio of the C2 specimen is identical to that of the S-vitrimer. Control group 3 (C3) is manufactured by the following method. DGEBA (1 g, 2.9 mmol), PPGDG (3.76 g, 5.8 mmol), DGCHD (0.84 g, 2.9 mmol), and 4-AFD (1.94 g, 7.8 mmol) were mixed, and the other process was conducted identically to the synthesis of the S-vitrimer. The synthesis route is described in Scheme S7. To check the ortho- and para-substitution effect of the hardener, C3 specimens were synthesized with 4-AFD instead of 2-AFD, differently from the S-vitrimer. The molar ratio is identical to that of an S-vitrimer (Table 1).

**Table 1. Molar Ratio of Each Sample**

	epoxy resin				hardener		
	DGEBA	PPGDG	PEGDG	DGCHD	2-AFD	4-AFD	EDA
S-vitrimer	1	2		1	2.7		
E-vitrimer	1				0.5		
P-vitrimer		1			0.5		
H-vitrimer				1	0.5		
C1 vitrimer	1	2		1			2.7
C2 vitrimer	1		2	1	2.7		
C3 vitrimer	1	2		1		2.7	

**2.3. Characterization Tests.** Fourier transform infrared (FTIR) spectra were recorded on a Vertex80V spectrometer from BRUKER. All samples were scanned 32 times at a resolution of 4  $\text{cm}^{-1}$ . Differential scanning calorimetry (DSC) analyses were performed using a Discovery DSC from the TA instrument. The temperature range was  $-30$  to 150 °C under nitrogen at a heating rate of 10 °C/min. Also, isothermal analysis was conducted at 150 °C under nitrogen to verify the termination of the curing reaction at 150 °C.

Thermogravimetric analysis (TGA) experiments were conducted with a Discovery TGA from TA Instrument under a nitrogen atmosphere at a heating rate of 10 °C/min from 25 to 600 °C to obtain the degradation temperature and overall thermal stability of the materials. Dynamic mechanical analysis (DMA) measurements were carried out on an SDTA861e from Mettler Toledo. The mode of deformation was applied in the tension mode with the sample size of 20 mm  $\times$  5 mm  $\times$  0.5 mm. The axial force amplitude was set to 10 N, and the displacement amplitude was set to 20  $\mu\text{m}$  with a single frequency mode (1 Hz frequency).

**2.4. Self-Healing Experiments.** To observe self-healing performance, tensile tests were performed using a Tinius-Olsen Model SST tensile tester with a 100 N load cell. The thickness of dumbbell-shaped specimens was approximately 2–2.5 mm. Tensile tests were performed with a 50 mm/min strain rate

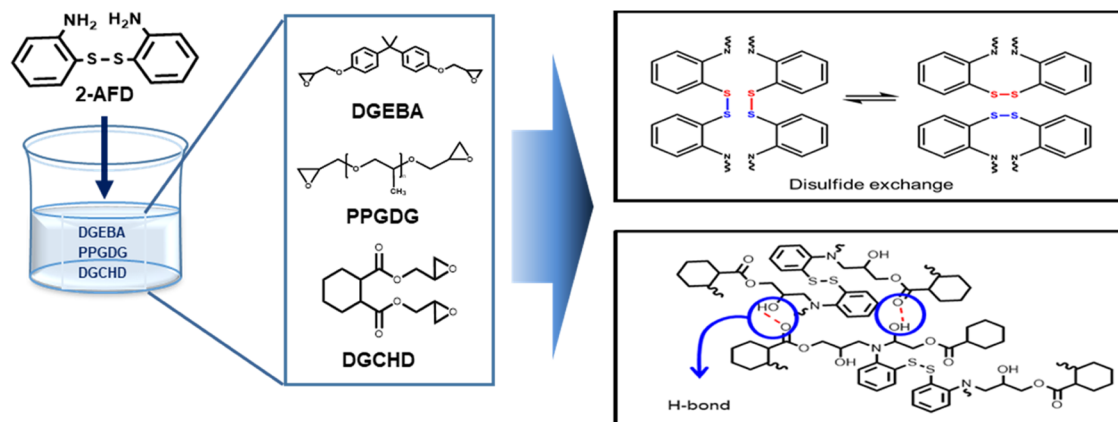


**Figure 2.** Synthesis of the self-healing epoxy disulfide vitrimer-like material (S-vitrimer). The vitrimer is healed through a disulfide exchange reaction and a hydrogen bond between carbonyl and hydroxyl groups.

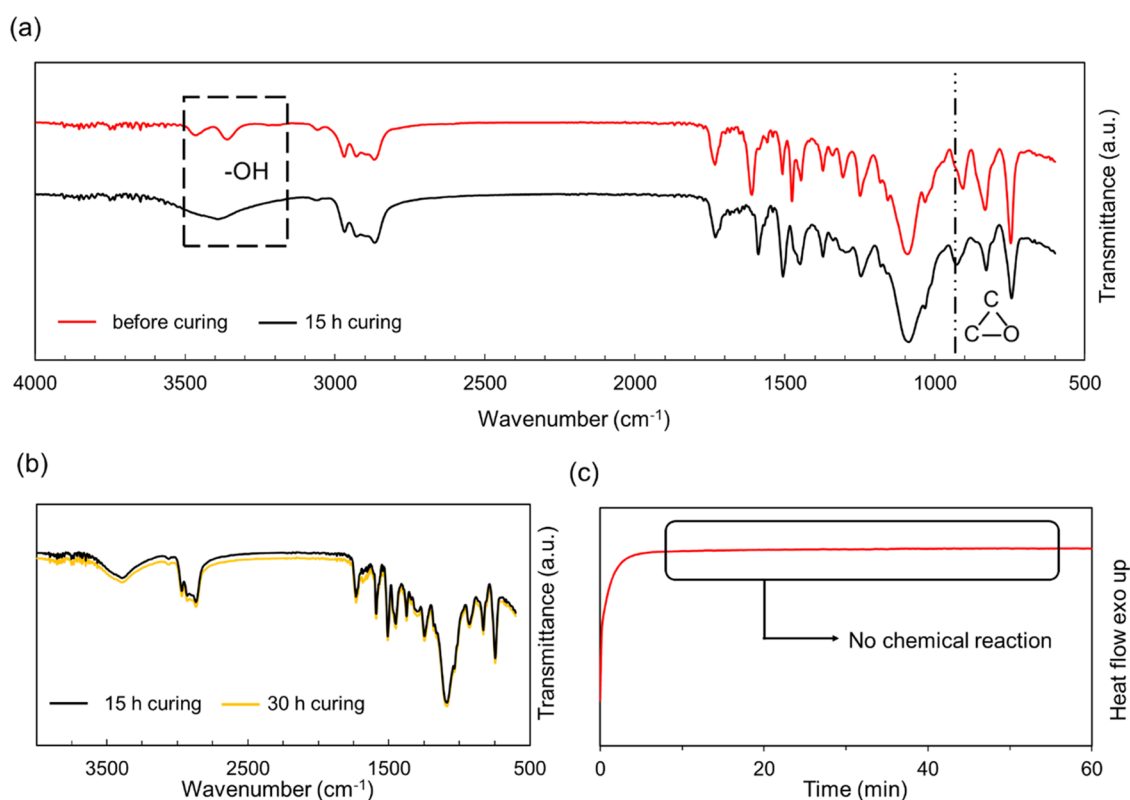


**Figure 3.** Curing analysis of the S-vitrimer. The FTIR graph of (a) uncured (red trace) and 15 h-cured (black trace) S-vitrimers and (b) 15 h (black trace)-cured and 30 h-cured (orange trace) vitrimer-like materials. (c) Isothermal DSC analysis of the S-vitrimer at 150 °C. Both (b) and (c) results suggested that the curing reaction was completed.

and a gauge length of 20 mm at room temperature (approximately 25 °C and 30% humidity).

Samples were healed through the following process. At first, the dumbbell-shaped sample was cut in half with a blade. Two parts were then reattached and left at room temperature for 24, 48, 72, and 96 h without applying any particular stimulus such as pressure, solvent, and light. Additionally, more experiments were conducted to study healing behavior at 40, 50, and 60 °C for 24 and 48 h without any external stimuli. The self-healing efficiency is defined as the ratio of pristine strength to the healed strength as expressed in eq 1.

$$\eta = \frac{\sigma_{\text{healed}}}{\sigma_{\text{original}}} \times 100 \quad (1)$$

### 3. RESULTS AND DISCUSSION

**3.1. Fabrication and Characterization of Epoxy Vitrimer-Like Materials.** As shown in Figure 2, elastomeric epoxy vitrimer-like materials named the S-vitrimer with a self-healing ability at room temperature were developed. 2-AFD was used to introduce the aromatic disulfide, which made the S-vitrimer self-healable at room temperature. DGCHD was added to employ the hydrogen bond formed by the carbonyl and hydroxyl group, which assists the aromatic disulfide in recovering the properties of the S-vitrimer. The intrinsic effect

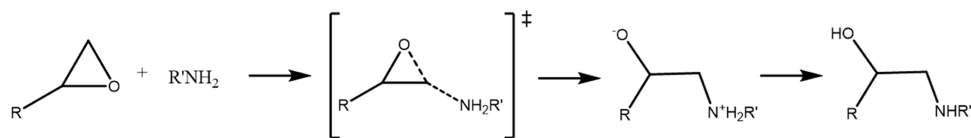


**Figure 4.** Mechanism of the epoxide ring and amine curing reaction.<sup>65</sup> The reaction occurs through the  $S_N2$  reaction, whose reactivity is mainly affected by steric hindrance. Reprinted with permission from ref 65. Copyright 2007 ACS Publications.

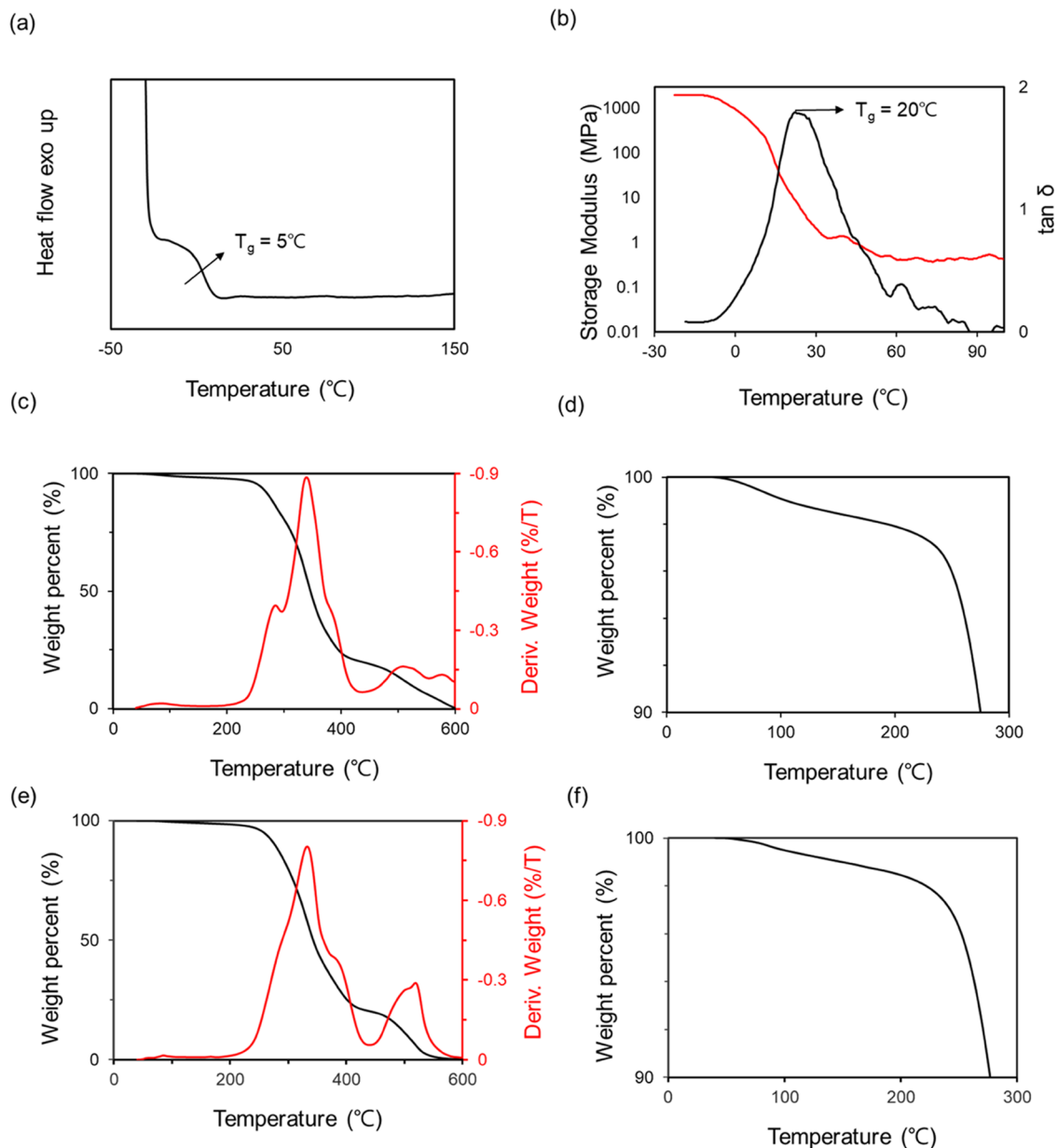


**Figure 5.** Thermal behavior of the S-vitrimer. (a) DSC graph of the S-vitrimer. (b) DMA graph of the S-vitrimer. The black line corresponds to the storage modulus, while the red line is the  $\tan \delta$  curve. The TGA graph of the S-vitrimer under (c, d) air and (e, f) nitrogen. The S-vitrimer began to thermally degrade at about 200 °C and degraded rapidly at about 340 °C. The S-vitrimer began to thermally degrade at about 200 °C and degraded rapidly at about 340 °C. The black line is the weight percent, and the red line is the derivative weight.

of disulfide and hydrogen on self-healing is examined thoroughly in Section 3.3. On the other hand, the main goal of PPGDG in the system was to decrease the  $T_g$  of the cured epoxy due to the linear aliphatic structure of PPGDG, promoting relatively higher mobility. Briefly, lower  $T_g$  was expected to increase mobility and hence the rate of self-healing.

FTIR analysis was performed to observe the chemical structure of the synthesized S-vitrimers. The structure of the S-vitrimer can be predicted by observing the range of spectra corresponding to the epoxide ring because the curing reaction of epoxy occurs through an epoxide ring-opening reaction. To check the epoxide ring, 890 to 950  $\text{cm}^{-1}$  spectra and 3300 to 3500  $\text{cm}^{-1}$  were investigated. As shown in Figure 3a, the

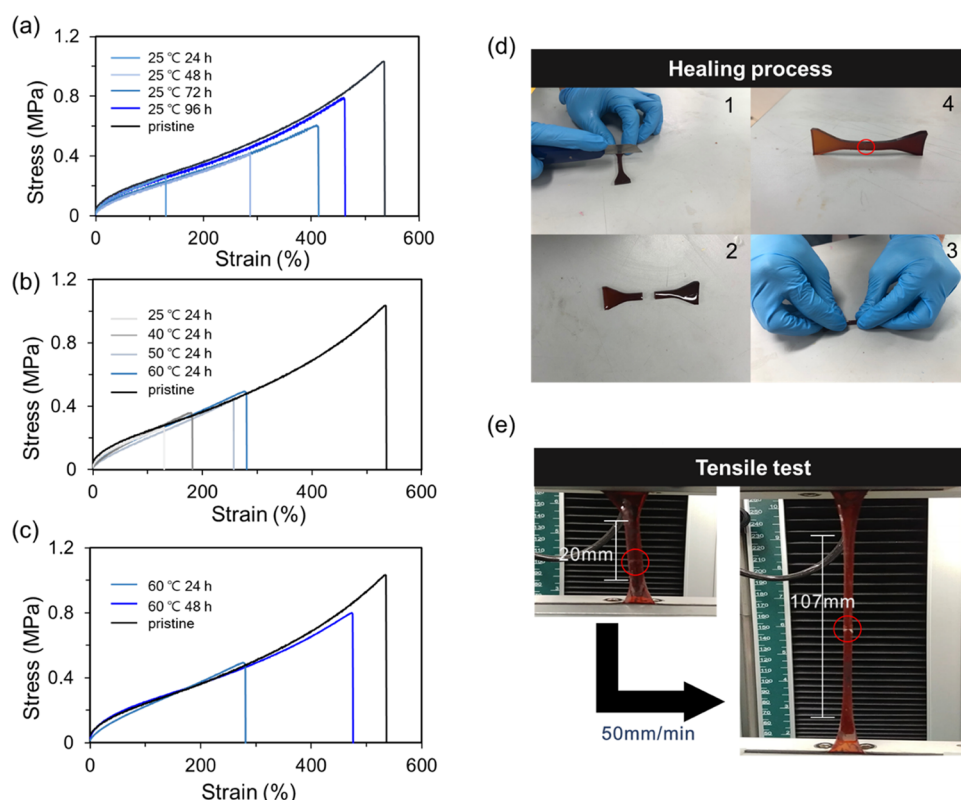


**Figure 6.** Healing behavior of the S-vitrimer. The stress–strain curve of the S-vitrimer (a) healed at room temperature for varying times. The S-vitrimer is healed 26, 41, 58, and 79% after 24, 48, 72, and 96 h, respectively. (b) Healed at varying temperatures for 24 h. The S-vitrimer is healed 28, 33, 42, and 46%, respectively. (c) Healed at 60 °C and showed an 80% healing efficiency after 48 h. (d) S-vitrimer was cut with a blade and then healed at room temperature, and then (e) tensile test with a 50 mm/min loading speed was performed.

reduction of 890 to 950  $\text{cm}^{-1}$  peaks was confirmed in FTIR spectra. Also, the appearance of the 3300 to 3500  $\text{cm}^{-1}$  peak is shown in Figure 3a. A reduction of the 890 to 950  $\text{cm}^{-1}$  area appeared due to the epoxide ring-opening reaction, and the appearance of a 3300–3500  $\text{cm}^{-1}$  wide peak indicates the hydrogen bond of the hydroxyl group. This result showed that the S-vitrimer was cured, considering the ring-opening reaction of the epoxide ring. Although the epoxide ring peak (890 to 950  $\text{cm}^{-1}$ ) did not disappear completely, it seems that the reaction was finished. Comparing FTIR spectra of the S-vitrimer cured for 30 h with the S-vitrimer cured for 15 h, the spectra of the 30 h-cured S-vitrimer are very similar to 15 h-cured, as shown in Figure 3b, which means that the vitrimer-like material no longer reacted after 15 h curing. DSC isothermal analysis also showed that the curing reaction was completed at 150 °C. If there were still epoxides remaining to react in the S-vitrimer, an exothermic peak would be observed. However, no exothermic behavior was found when the S-vitrimer was left at 150 °C for 1 h in DSC, as shown in Figure 3c. The S-vitrimer did not show any thermal behavior at 150 °C, which means that the curing reaction of the S-vitrimer did not occur anymore after 15 h curing. Figure 3b,c proves that the curing reaction of the S-vitrimer was completed at 150 °C.

It is difficult to measure the degree of curing ( $\alpha$ ) in FTIR by simply comparing the absolute absorbance value because the shape of the spectrum changes after the ring-opening reaction. Therefore, the peak should be normalized with respect to the reference peak that is not engaged in the curing reaction. In this paper, the ether bond was used as a reference peak because

the ether bond does not attend the curing reaction. The degree of curing ( $\alpha$ ) was calculated by measuring the height of the peak as described in detail. First, find the epoxide ring peak (890 to 950  $\text{cm}^{-1}$ ) and the ether bond peak (1000 to 1100  $\text{cm}^{-1}$ ). Next, the baseline was drawn between the local minimum, and the height of the peak was measured by gauging the height between the peak point and the baseline (Figure S1). Then, the degree of curing can be evaluated as in eq 2

$$\alpha = \left[ 1 - \frac{(h_{\text{after}}^{\text{epoxy}}/h_{\text{after}}^{\text{ether}})}{(h_{\text{before}}^{\text{epoxy}}/h_{\text{before}}^{\text{ether}})} \right] \times 100 (\%) \quad (2)$$

where  $h_{\text{before}}^{\text{epoxy}}$  is the height of the epoxide ring before the curing reaction,  $h_{\text{before}}^{\text{ether}}$  is the height of the ether bond before the curing reaction,  $h_{\text{after}}^{\text{epoxy}}$  is the height of the epoxide ring after the curing reaction, and  $h_{\text{after}}^{\text{ether}}$  is the height of the ether bond after the curing reaction. As presented in Table S1, the degree of curing for the S-vitrimer is found as 47.2%.

The aforementioned curing behavior of the vitrimer-like material can be attributed to the steric hindrance of PPGDG. To prove this effect, a 2-AFD hardener was cured with only one of the resins among DGEBA, PPGDG, and DGCHD, which were named E-vitrimer, P-vitrimer, and H-vitrimer, respectively. In the case of the E-vitrimer and H-vitrimer, it is observed that the peak between 890 and 950  $\text{cm}^{-1}$  almost disappears, as shown in Figure S3. By the same calculation method of the curing degree, it was found that curing is completed 70 and 90% in the E-vitrimer and H-vitrimer, respectively. In contrast, the 890 to 950  $\text{cm}^{-1}$  peak of the P-vitrimer remained still noticeable after curing, and the degree

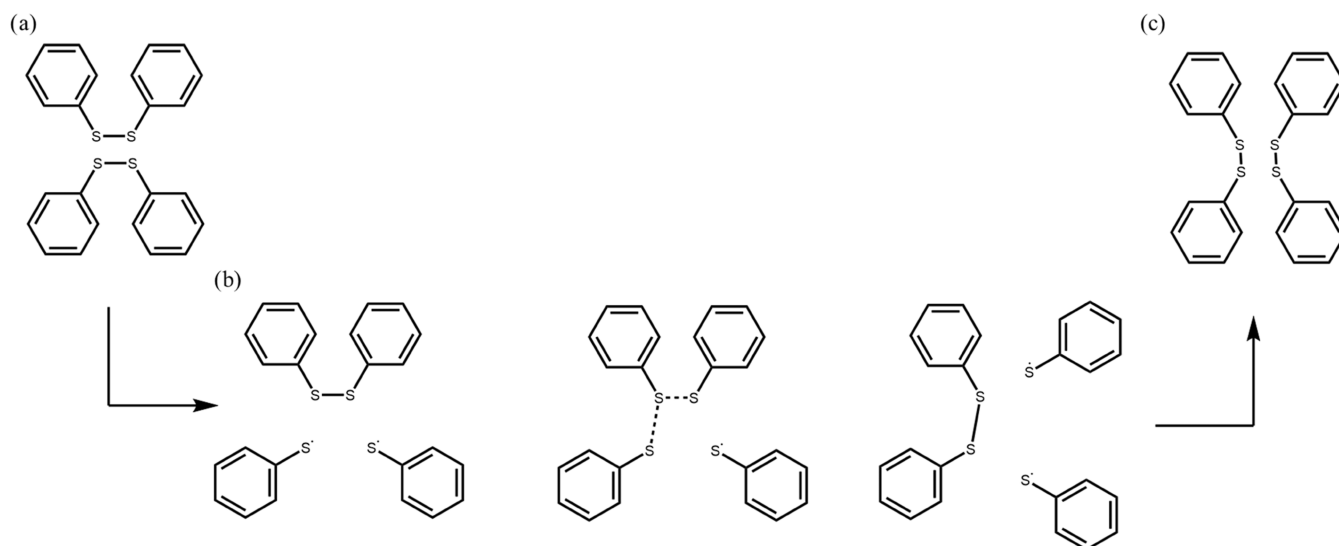


**Figure 7.** [2 + 1] radical-mediated reaction mechanism of the disulfide exchange reaction.<sup>67</sup> The radical is stabilized due to the delocalization of the radical electron caused by the aromatic ring bonded to sulfide. (a) Aromatic disulfide structure before the exchange reaction. (b) Aromatic disulfide exchange reaction through hemolysis. (c) Result of the exchange reaction. Reprinted with permission from ref 67. Copyright 2016 Elsevier.

of curing ended at only 26% (Table S1). It is concluded that the long-chained structure of PPGDG increases steric hindrance and hampers the reaction. The decrease in the degree of reaction is attributed to the  $S_N2$  reaction during epoxy curing,<sup>64,65</sup> which is significantly affected by steric hindrance, as shown in Figure 4. It is the reason why the epoxide ring stretching peak did not disappear completely in the S-vitrimer, although the reaction ended at 150 °C.

TGA experiments were carried out from 40 to 600 °C under a nitrogen and air atmosphere to measure the thermal stability in the inert and normal states. Thermal stability can be obtained by analyzing the derivative weight, as shown in Figure 5c,e. As shown in Figure 5c, thermal degradation began around 200 °C, which means that the S-vitrimer should avoid being left around 200 °C under air since it begins to degrade afterward. A 5% weight reduction was found at 256 °C and a 10% weight reduction was shown at 275 °C, as shown in Figure 5d. The S-vitrimer started degrading most rapidly at around 332 °C. The thermal behavior of the S-vitrimer under nitrogen was very similar to the case under air, as shown in Figure 5e,f. It is inferred that the S-vitrimer was degraded by heat rather than the external air effect. As shown in Figure 5a, the  $T_g$  value of the S-vitrimer is 5 °C by DSC analysis. As shown in Figure 5b, the  $T_g$  value of the S-vitrimer is 20 °C by DMA analysis. Generally, there is a difference in the  $T_g$  value in DSC and DMA. It is because  $T_g$  is not a specific point like melting and boiling temperature, but it is a temperature range between the first-order and second-order phase transition. The  $T_g$  value changes according to various parameters such as the heating rate and frequency, leading to the difference. The DSC is a static method where the energy difference is measured to identify the glass transition temperature because when the transition occurs, the heat capacity of polymers changes. On the other hand, it is also possible to analyze glass transition temperature through DMA in terms of molecular mobility because of the free volume increase in the  $T_g$  value. It is a dynamic method by which the viscoelastic modulus is measured. The storage modulus, related to elasticity, decreases, while the loss modulus, related to viscosity, increases when heating in the glass transition temperature range. It is because

the polymer changes into the rubbery phase due to the polymer chain uncoiling phenomenon when the temperature is higher than the  $T_g$  value.

**3.2. Self-Healing Test.** To confirm the performance of self-healing, self-healing experiments were conducted as follows. The S-vitrimer was cut into two pieces, and then two pieces were directly put into contact at room temperature without any external force. The reattached S-vitrimer was left at room temperature for various durations, and strength was measured through the tensile test. Healed strength obtained by the tensile test was compared with pristine strength to evaluate the self-healing efficiency of the S-vitrimer, as shown in Figure 6.

The S-vitrimer showed 26, 41, 58, and 79% healing efficiencies when healed for 24, 48, 72, and 96 h, respectively, as shown in Figure 6a. These results demonstrated that healing efficiency increases as the healing time increases. The longer healing time means that the time for the disulfide exchange reaction increases. It confirms that as the S-vitrimer undergoes a disulfide exchange reaction for a longer time, the S-vitrimer heals itself more. For instance, the healing efficiency of the S-vitrimer reached about 80% after healing for 96 h at room temperature.

The S-vitrimer can be healed at room temperature due to the aromatic disulfide bond and the hydrogen bond. Herein, the aromatic disulfide bond exists in 2-AFD, and the hydrogen bond comes from the hydroxyl group and carboxylic group of DGCHD. The hydroxyl group is formed as a result of the epoxide ring-opening reaction. The role of the aromatic disulfide bond and the hydrogen bond in healing is investigated in detail in Section 3.3.

The aromatic disulfide bond undergoes an exchange reaction at room temperature, even in a solid state. It leads to an exchange reaction in a low-energy environment like room temperature. There are two reasons why aromatic disulfide exchange reactions can occur at room temperature. First, the sulfenyl radical created when the exchange reaction occurs is stabilized due to the delocalization of the free radical<sup>66,67</sup> (Figure 7). Additionally, due to the increase in the number of antibonding electron quanta in molecular orbitals, dissociation

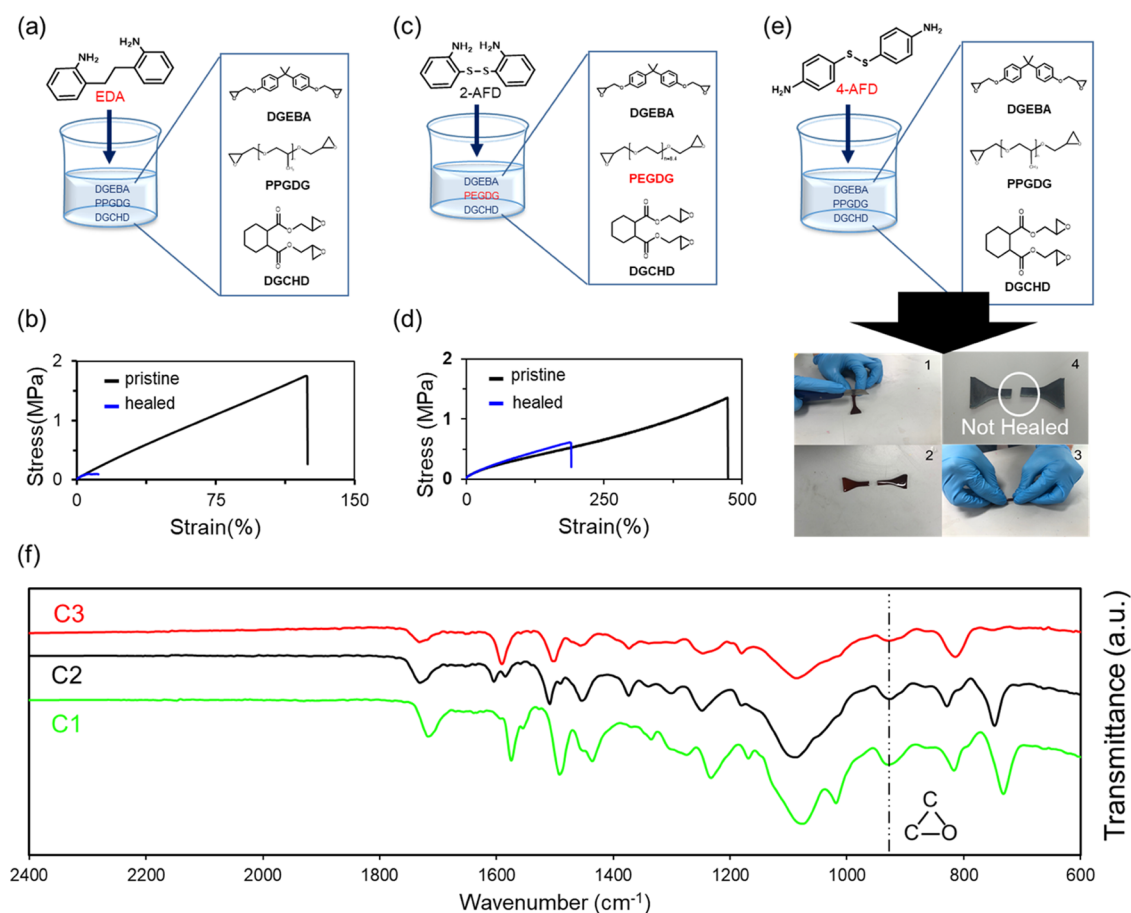


**Figure 8.** (a) Synthesis and starting materials of control group C1 without disulfide. (b) Stress–strain curve of C1, which showed a 6.4% healing efficiency. (c) Synthesis and starting materials of control group C2 without a pendant group of the soft segment. (d) Stress–strain curve of C2, which showed a 45% healing efficiency. (e) Synthesis and starting materials of control group C3 with a para-substitution hardener. C3 did not show self-healing behavior. (f) FTIR graph of control groups. The graph shows 890 to 950  $\text{cm}^{-1}$  corresponding to the epoxide ring that remained in C1 (green trace), C2 (black trace), and C3 (red trace).

of the S–S bond occurs more quickly, making exchange reactions occur at room temperature.<sup>66</sup> The working mechanism of the aromatic disulfide exchange reaction in the healing process can be explained as follows. The aromatic disulfide exchange reaction works as a chemical operator so that the chemical bonds broken under fracture can be reconnected and recovered to their original state. As a result of these recovered bonds at the fracture surface, the material state can go back to its original properties.<sup>17,18</sup>

To initiate the disulfide exchange reaction, the glass transition temperature ( $T_g$ ) of the aromatic disulfide vitrimer must be lower than room temperature because the disulfide exchange reaction can occur when the vitrimer has enough mobility.<sup>68</sup> Mobility allows the disulfide bond exchange, owing to the collision between S atoms, as there would be no collision in the molecule at a temperature lower than  $T_{g}$ . Through DSC and DMA, it is confirmed that  $T_g$  of the S-vitrimer is lower than room temperature, which means that the disulfide exchange reaction can take place at room temperature as well as the healing process. As a result of DSC analysis, it is found that the  $T_g$  value of the S-vitrimer is 5 °C, as shown in Figure 5a. Also, through the DMA experiment, the  $T_g$  value of the S-vitrimer is detected as 20 °C, as shown in Figure 5b. When the S-vitrimer was left in the refrigerator at 5 °C, self-healing behavior was not observed since the disulfide exchange reaction did not get activated below  $T_g$ .

The hydrogen bond also allows the S-vitrimer to be healed at room temperature efficiently within their weak bonding structure. It is easy to break and reform hydrogen bonds reversibly, allowing a more efficient and easier healing mechanism. As shown in Figure 3a, a 3300–3500  $\text{cm}^{-1}$  wide peak does not exist before curing. After curing, a wide peak appears in the range of 3300–3500  $\text{cm}^{-1}$ . The formation of a broad peak around 3300–3500  $\text{cm}^{-1}$  infers that a hydrogen bond was created after the curing reaction.

In addition, the S-vitrimer was healed at different temperatures to understand the effect of temperature on the healing efficiency better. The S-vitrimer showed 28, 33, 42, and 46% healing efficiencies at room temperature, 40, 50, and 60 °C, as shown in Figure 6b. The increased healing efficiencies are attributed to the increased material mobility. As the temperature increases, the mobility also increases, leading to more efficient healing of the S-vitrimer. It should be pointed out that the healing efficiency reaches nearly 80% after healing for 48 h at 60 °C, as shown in Figure 6c. Furthermore, the S-vitrimer showed such a high healing efficiency at 60 °C in a shorter time than the same healing process at room temperature.

**3.3. Control Experiments.** Three control experiments were performed by changing one parameter each time to investigate the key factors that affect self-healing behavior. All control groups were cured for 15 h at 150 °C, and the curing reaction was followed by FTIR analysis, as shown in Figure 8f.



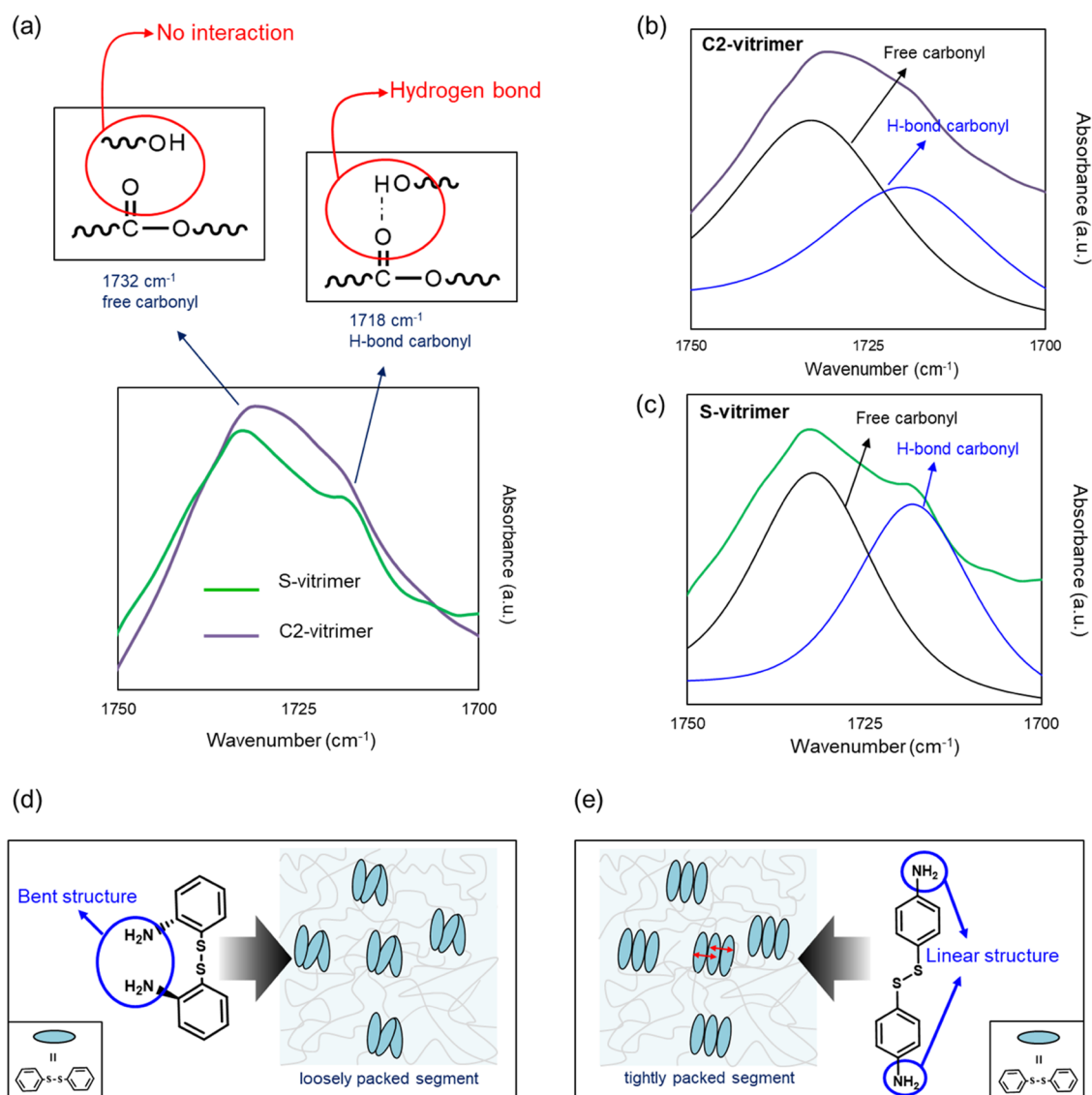


**Figure 9.** Molecular structure of control vitrimer-like materials. (a) ATR-FTIR spectra of the S-vitrimer and the C2 experiment. In the spectra, 1732 cm<sup>-1</sup> corresponds to free carbonyl (without interaction with the hydroxyl group) and 1718 cm<sup>-1</sup> corresponds to hydrogen-bonded carbonyl. The carbonyl region of the FTIR spectrum is resolved into free and hydrogen-bonded carbonyl peaks in (b) C2 and (c) S-vitrimer. The molecular structure of (d) S-vitrimer, which possesses a bent structure of a hardener, has higher free volume and loosely packed segment. (e) C3 (right), which possesses a quasi-linear structure of a hardener, has lower free volume and a tightly packed segment.

After the curing reaction, 890 to 950 cm<sup>-1</sup> peaks remained in C1, C2, and C3, similar to the S-vitrimer, and the degree of curing was also found to be similar (Table S1). Within the similar degree of curing of the S-vitrimer and control samples, it is deduced that the healing behavior of these control groups can be compared with the S-vitrimer. The control groups were also analyzed under isothermal DSC analysis (Figure S4a,c,e) and did not show any exothermic peak corresponding to the further curing reaction. Such a result indicated that the curing reaction of three control groups was completed at 150 °C. In other words, the control groups were also not fully cured, similar to the S-vitrimer. Self-healing experiments of three control groups were performed identically to the process mentioned above, and all self-healing experiments were conducted at room temperature for 96 h.

First, epoxy materials without disulfide (C1) were synthesized to explore the disulfide and hydrogen bond effect. C1 was fabricated using an EDA hardener instead of a 2-AFD

hardener used in the S-vitrimer (Figure 8a). It is possible to study both disulfide and hydrogen bond effects with EDA because it has a CH<sub>2</sub>-CH<sub>2</sub> bond instead of a S-S bond in AFD.

The result of the C1 experiment showed a 6.4% healing efficiency (Figure 8b). This result indicated that the absence of disulfide led to a major reduction in self-healing behavior. At the same time, it indicated that hydrogen bonds play a role in self-healing since there is still healing in the C1 sample with only hydrogen bonds in its structure. Hence, the hydrogen bond is found to be capable of performing self-healing in the absence of disulfide bonds, wherein the efficiency is much less than the S-vitrimer due to the absence of disulfide bonds. The hydrogen bond effect was hereby examined through both FTIR results (Figure 3a and control group C1). Meanwhile, DSC analysis showed that C1 has a *T<sub>g</sub>* value of 15 °C lower than room temperature (Figure S4b).

Next, PEGDG was employed instead of PPGDG to investigate the effect of the pendant group of the soft segment, which is related to crystallinity (Figure 8c). As shown in Figure 8c, PEGDG does not have a CH<sub>3</sub> substituent that exists in PPGDG. It was possible to explore the effect of methyl substituent branching by comparing PPGDG and PEGDG, as they both have about eight repeating units. Moreover, the  $T_g$  value of C2 is around 6 °C (Figure S4d), which is comparable to the  $T_g$  value of the S-vitrimer. Therefore, the only difference between the S-vitrimer and C2 is the soft segment unit, PPGDG, and PEGDG.

It was found that the healing efficiency of C2 was only 45% (Figure 8d), implying the importance of the extra methyl substituent of PPGDG on self-healing performance. Such a decrease in the healing efficiency of C2 is attributed to the pendant group<sup>18</sup> of the resulting epoxy vitrimer-like materials, as PEGDG has higher crystallinity than PPGDG due to the substituent. It was reported that there is a chain branching effect in polyethylene,<sup>69</sup> such that the more methyl substituent polyethylene has, the lower crystallinity is observed in the structure, as shown in Scheme S8.

To verify the existence of a pendant group, the 1700 to 1750 cm<sup>-1</sup> peak corresponding to the carbonyl group was analyzed through attenuated total reflection-Fourier transform infrared spectroscopy (ATR-FTIR) (Figure 9a). A peak at 1732 cm<sup>-1</sup> is observed, corresponding to free carbonyl without a hydrogen bond with a hydroxyl group. The peak at 1718 cm<sup>-1</sup> is related to the hydrogen-bonded carbonyl group.<sup>70</sup> The carbonyl region of the FTIR spectrum is resolved into free and hydrogen-bonded carbonyl to compare the number of the carbonyl group with and without hydrogen bonds by evaluating the area below the curves (Figure 9b,c). The results exhibited that the number of the carbonyl group with hydrogen bonds reached 87% of free carbonyl in the S-vitrimer. In the case of C2, the number of the hydrogen-bonded carbonyl group just ended up at 66.0% of the free carbonyl group (Table S3). This is attributed to the soft segment of the S-vitrimer having a CH<sub>3</sub> pendant group, resulting in less crystallinity, which promotes the hydrogen bond. As a result, the S-vitrimer having higher healing efficiency than C2 signifies the role of hydrogen bonds.

To ensure the effect of the hardener, another control experiment was conducted. In this last control experiment, 2-AFD *ortho*-substitution was replaced with 4-AFD *para*-substitution (Figure 9e). The DSC result showed that C3 has a  $T_g$  value of 25 °C (Figure S4f). Self-healing experiments were conducted at 60 °C as well as at room temperature. Even though 60 °C is far higher than  $T_g$  in which C3 has enough mobility, there was no self-healing behavior observed similar to the case at room temperature. It can be explained that tightly packed segments hindered self-healing behavior regardless of mobility. Kim et al. also reported that tightly packed segments affect self-healing behavior in a negative way.<sup>18</sup> As shown in Figure 9d,e, an *ortho*-substituted hardener with a bent structure generates a loosely packed conformation, while a *para*-substituted hardener with a quasi-linear structure lets molecules be tightly packed. Therefore, it clarifies the lower  $T_g$  value of the S-vitrimer (Table S2) as it is less packed and has more free volume compared to C3. In summary, it is concluded that a highly packed structure prevents the healing mechanism in self-healing materials.

## 4. CONCLUSIONS

In this paper, epoxy-based self-healing materials (S-vitrimer) that can be healed without any external stimuli were synthesized. To the best knowledge of the authors, it is the first time that an epoxy network healable without any stimuli at room temperature is reported. The S-vitrimer was characterized by FTIR, DSC, DMA, and TGA. Also, various control experiments were conducted to describe the working mechanism of the overall self-healing process in detail.

This study explored that the S-vitrimer can be healed at even room temperature with an aromatic disulfide exchange reaction and a hydrogen bond. When the S-vitrimer was left in contact for a longer time, a higher healing efficiency was observed. In particular, the S-vitrimer recovered about 80% of the pristine strength at room temperature at 96 h and 60 °C in 48 h.

Finally, three control experiments were conducted to demonstrate the parameters affecting the self-healing behavior. First, the C1 experiment without disulfide was performed, and a 6.4% healing efficiency was achieved. Through C1, it was found that the disulfide exchange reaction played an essential role in self-healing behavior, but the importance of a hydrogen bond is also pointed out in healing behavior. C2 experiments without a pendant group were conducted, and the sample recovered 45% of its original strength after self-healing. The pendant group implements more hydrogen bonds to the S-vitrimer, which directly affects the self-healing behavior. Finally, C3 was synthesized with a different hardener formed of *para*-substitution in which healing behavior is not observed. C3 results suggested that a tightly packed structure prevents high healing efficiency. Optimization of such a system offers a new generation of epoxy-based composite materials with the capability of self-healing even at room temperature. In the future, care can be taken to further enhance mechanical strength.

## ■ ASSOCIATED CONTENT

### SI Supporting Information

The Supporting Information is available free of charge at <https://pubs.acs.org/doi/10.1021/acsomega.2c04559>.

Synthesis route of S-vitrimer; synthesis routes and dsc results of control groups; the amount of hydrogen bonds in C2 vitrimer; method to calculate the height of peak; FTIR graph of S-vitrimer before curing (black line) and after curing (red line); isothermal DSC analysis; calculating degree of curing based on the area under FTIR curve, and composition of self-healing vitrimers and synthesis results (PDF)

## ■ AUTHOR INFORMATION

### Corresponding Author

Gun Jin Yun – Department of Aerospace Engineering, Seoul National University, Seoul 08826, South Korea; Institute of Advanced Aerospace Engineering Technology, Seoul National University, Seoul 08826, South Korea; [orcid.org/0000-0001-8387-3613](https://orcid.org/0000-0001-8387-3613); Email: [gunjin.yun@snu.ac.kr](mailto:gunjin.yun@snu.ac.kr)

### Authors

Geonwoo Kim – Department of Aerospace Engineering, Seoul National University, Seoul 08826, South Korea  
Cigdem Caglayan – Department of Aerospace Engineering, Seoul National University, Seoul 08826, South Korea

Complete contact information is available at:

<https://pubs.acs.org/10.1021/acsomega.2c04559>

## Notes

The authors declare no competing financial interest.

## ACKNOWLEDGMENTS

This work was supported by the Institute of Engineering Research at Seoul National University. The authors are grateful for their support. This material is also based upon work supported by the Air Force Office of Scientific Research under award number FA2386-20-1-4067. This work was also supported by the BK21 Program funded by the Ministry of Education (MOE, Korea) and the National Research Foundation of Korea (NRF-419990513944). The authors are grateful for their support.

## REFERENCES

- (1) Williams, G.; Trask, R.; Bond, I. A self-healing carbon fibre reinforced polymer for aerospace applications. *Composites, Part A* **2007**, *38*, 1525–1532.
- (2) Coope, T. S.; Turkenburg, D. H.; Fischer, H. R.; Luterbacher, R.; Van Bracht, H.; Bond, I. P. Novel Diels-Alder based self-healing epoxies for aerospace composites. *Smart Mater. Struct.* **2016**, *25*, No. 084010.
- (3) Yu, K. H.; Du, H. X.; Xin, A.; Lee, K. H.; Feng, Z. Z. R.; Masri, S. F.; Chen, Y.; Huang, G. L.; Wang, Q. M. Healable, memorizable, and transformable lattice structures made of stiff polymers. *NPG Asia Mater.* **2020**, *12*, No. 26.
- (4) Srinivas, P. N. S.; Babu, P. R.; Balakrishna, B. Material characterization and optimization of CNT-reinforced aluminum (AA7075) functionally graded material processed by ultrasonic cavitation. *Funct. Compos. Struct.* **2020**, *2*, No. 045002.
- (5) Cao, Y.; Tan, Y. J.; Li, S.; Lee, W. W.; Guo, H. C.; Cai, Y. Q.; Wang, C.; Tee, B. C. K. Self-healing electronic skins for aquatic environments. *Nat. Electron.* **2019**, *2*, 75–82.
- (6) Kang, J.; Son, D.; Wang, G. J. N.; Liu, Y.; Lopez, J.; Kim, Y.; Oh, J. Y.; Katsumata, T.; Mun, J.; Lee, Y.; et al. Tough and water-insensitive self-healing elastomer for robust electronic skin. *Adv. Mater.* **2018**, *30*, No. 1706846.
- (7) Khatib, M.; Zohar, O.; Saliba, W.; Haick, H. A Multifunctional Electronic Skin Empowered with Damage Mapping and Autonomic Acceleration of Self-Healing in Designated Locations. *Adv. Mater.* **2020**, *32*, No. 2000246.
- (8) Terryn, S.; Brancart, J.; Lefeber, D.; Van Assche, G.; Vanderborcht, B. Self-healing soft pneumatic robots. *Sci. Rob.* **2017**, *2*, No. ean4268.
- (9) Markvicka, E. J.; Bartlett, M. D.; Huang, X. N.; Majidi, C. An autonomously electrically self-healing liquid metal-elastomer composite for robust soft-matter robotics and electronics. *Nat. Mater.* **2018**, *17*, 618–624.
- (10) Pena-Francesch, A.; Jung, H.; Demirel, M. C.; Sitti, M. Biosynthetic self-healing materials for soft machines. *Nat. Mater.* **2020**, *19*, 1230–1235.
- (11) Turkenburg, D.; Fischer, H. Diels-Alder based, thermoreversible cross-linked epoxies for use in self-healing composites. *Polymer* **2015**, *79*, 187–194.
- (12) Lin, C.; Ge, H.; Wang, T.; Huang, M.; Ying, P.; Zhang, P.; Wu, J.; Ren, S.; Levchenko, V. A self-healing and recyclable polyurethane/halloysite nanocomposite based on thermoreversible Diels-Alder reaction. *Polymer* **2020**, *206*, No. 122894.
- (13) Li, S.; Zuo, C.; Zhang, Y.; Wang, J.; Gan, H.; Li, S.; Yu, L.; Zhou, B.; Xue, Z. Covalently cross-linked polymer stabilized electrolytes with self-healing performance via boronic ester bonds. *Polym. Chem.* **2020**, *11*, 5893–5902.
- (14) Cromwell, O. R.; Chung, J.; Guan, Z. Malleable and self-healing covalent polymer networks through tunable dynamic boronic ester bonds. *J. Am. Chem. Soc.* **2015**, *137*, 6492–6495.
- (15) Pepels, M.; Filot, I.; Klumperman, B.; Goossens, H. Self-healing systems based on disulfide–thiol exchange reactions. *Polym. Chem.* **2013**, *4*, 4955–4965.
- (16) Xu, Y.; Chen, D. A novel self-healing polyurethane based on disulfide bonds. *Macromol. Chem. Phys.* **2016**, *217*, 1191–1196.
- (17) Rekondo, A.; Martin, R.; de Luzuriaga, A. R.; Cabañero, G.; Grande, H. J.; Odriozola, I. Catalyst-free room-temperature self-healing elastomers based on aromatic disulfide metathesis. *Mater. Horiz.* **2014**, *1*, 237–240.
- (18) Kim, S. M.; Jeon, H.; Shin, S. H.; Park, S. A.; Jegal, J.; Hwang, S. Y.; Oh, D. X.; Park, J. Superior toughness and fast self-healing at room temperature engineered by transparent elastomers. *Adv. Mater.* **2018**, *30*, No. 1705145.
- (19) Wang, P.; Yang, L.; Dai, B.; Yang, Z.; Guo, S.; Gao, G.; Xu, L.; Sun, M.; Yao, K.; Zhu, J. A self-healing transparent polydimethylsiloxane elastomer based on imine bonds. *Eur. Polym. J.* **2020**, *123*, No. 109382.
- (20) Hu, J.; Mo, R.; Sheng, X.; Zhang, X. A self-healing polyurethane elastomer with excellent mechanical properties based on phase-locked dynamic imine bonds. *Polym. Chem.* **2020**, *11*, 2585–2594.
- (21) Zhou, Z.; Zeng, Y.; Yu, C.; Chen, H.; Zhang, F. Mechanically robust, intrinsically self-healing crosslinked polymer enabled by dynamic urea bond exchange reaction. *Smart Mater. Struct.* **2020**, *29*, No. 115041.
- (22) Ying, H.; Zhang, Y.; Cheng, J. Dynamic urea bond for the design of reversible and self-healing polymers. *Nat. Commun.* **2014**, *5*, No. 3218.
- (23) Fu, Q.; Yan, Q.; Jiang, X.; Fu, H. Heat driven self-healing isocyanate-based crosslinked three-arm Star-shaped polyglycolide based on dynamic transesterification. *React. Funct. Polym.* **2020**, *146*, No. 104440.
- (24) Yang, X.; Guo, L.; Xu, X.; Shang, S.; Liu, H. A fully bio-based epoxy vitrimer: Self-healing, triple-shape memory and reprocessing triggered by dynamic covalent bond exchange. *Mater. Des.* **2020**, *186*, No. 108248.
- (25) Yang, Y.; Pei, Z.; Zhang, X.; Tao, L.; Wei, Y.; Ji, Y. Carbon nanotube–vitrimer composite for facile and efficient photo-welding of epoxy. *Chem. Sci.* **2014**, *5*, 3486–3492.
- (26) Bonab, V. S.; Karimkhani, V.; Manas-Zloczower, I. Ultra-Fast Microwave Assisted Self-Healing of Covalent Adaptive Polyurethane Networks with Carbon Nanotubes. *Macromol. Mater. Eng.* **2019**, *304*, No. 1800405.
- (27) Wang, Y.; Liu, Q.; Li, J.; Ling, L.; Zhang, G.; Sun, R.; Wong, C.-P. UV-triggered self-healing polyurethane with enhanced stretchability and elasticity. *Polymer* **2019**, *172*, 187–195.
- (28) Zheng, H.; Wang, S.; Lu, C.; Ren, Y.; Liu, Z.; Ding, D.; Wu, Z.; Wang, X.; Chen, Y.; Zhang, Q. Thermal, near-infrared light, and amine solvent triple-responsive recyclable imine-type vitrimer: shape memory, accelerated photohealing/welding, and destructing behaviors. *Ind. Eng. Chem. Res.* **2020**, *59*, 21768–21778.
- (29) Caruso, M. M.; Blaiszik, B. J.; White, S. R.; Sottos, N. R.; Moore, J. S. Full recovery of fracture toughness using a nontoxic solvent-based self-healing system. *Adv. Funct. Mater.* **2008**, *18*, 1898–1904.
- (30) Chang, K.; Jia, H.; Gu, S.-Y. A transparent, highly stretchable, self-healing polyurethane based on disulfide bonds. *Eur. Polym. J.* **2019**, *112*, 822–831.
- (31) Ling, L.; Li, J.; Zhang, G.; Sun, R.; Wong, C.-P. Self-healing and shape memory linear polyurethane based on disulfide linkages with excellent mechanical property. *Macromol. Res.* **2018**, *26*, 365–373.
- (32) Mai, V.-D.; Shin, S.-R.; Lee, D.-S.; Kang, I. Thermal healing, reshaping and ecofriendly recycling of epoxy resin crosslinked with Schiff base of vanillin and hexane-1, 6-diamine. *Polymers* **2019**, *11*, No. 293.
- (33) Jiang, Y.; Qiu, L.; Juarez-Perez, E. J.; Ono, L. K.; Hu, Z.; Liu, Z.; Wu, Z.; Meng, L.; Wang, Q.; Qi, Y. Reduction of lead leakage from damaged lead halide perovskite solar modules using self-healing polymer-based encapsulation. *Nat. Energy* **2019**, *4*, 585–593.

- (34) Neisiany, R. E.; Lee, J. K. Y.; Khorasani, S. N.; Ramakrishna, S. Towards the development of self-healing carbon/epoxy composites with improved potential provided by efficient encapsulation of healing agents in core-shell nanofibers. *Polym. Test.* **2017**, *62*, 79–87.
- (35) Zhao, Y.; Fickert, J.; Landfester, K.; Crespy, D. Encapsulation of self-healing agents in polymer nanocapsules. *Small* **2012**, *8*, 2954–2958.
- (36) Cinquin, J.; Colin, X.; Fayolle, B.; Mille, M.; Terekhina, S.; Chocinski-Arnault, L.; Gigliotti, M.; Grandidier, J.-C.; Lafarie-Frenot, M.-C.; Minervino, M.; et al. Thermo-oxidation behaviour of organic matrix composite materials at high temperatures. *Adv. Aircr. Spacecr. Sci.* **2016**, *3*, 171–195.
- (37) Shokrieh, M.; Kondori, M. S. Effects of adding graphene nanoparticles in decreasing of residual stresses of carbon/epoxy laminated composites. *Compos. Mater. Eng.* **2020**, *2*, 53–64.
- (38) Wang, W.; Luo, M.; Yao, W.; Ma, M.; Pullarkat, S. A.; Xu, L.; Leung, P.-H. Catalyst-free and Solvent-free Cyanosilylation and Knoevenagel Condensation of Aldehydes. *ACS Sustainable Chem. Eng.* **2019**, *7*, 1718–1722.
- (39) Zou, Y.; Fang, L.; Chen, T.; Sun, M.; Lu, C.; Xu, Z. Near-infrared light and solar light activated self-healing epoxy coating having enhanced properties using MXene flakes as multifunctional fillers. *Polymers* **2018**, *10*, No. 474.
- (40) Krishnakumar, B.; Sanka, R. S. P.; Binder, W. H.; Park, C.; Jung, J.; Parthasarthy, V.; Rana, S.; Yun, G. J. Catalyst free self-healable vitrimer/graphene oxide nanocomposites. *Composites, Part B* **2020**, *184*, No. 107647.
- (41) Capelot, M.; Montarnal, D.; Tournilhac, F.; Leibler, L. Metal-catalyzed transesterification for healing and assembling of thermosets. *J. Am. Chem. Soc.* **2012**, *134*, 7664–7667.
- (42) Li, Z.-J.; Zhong, J.; Liu, M.-C.; Rong, J.-C.; Yang, K.; Zhou, J.-Y.; Shen, L.; Gao, F.; He, H.-F. Investigation on self-healing property of epoxy resins based on disulfide dynamic links. *Chin. J. Polym. Sci.* **2020**, *38*, 932–940.
- (43) Denissen, W.; Winne, J. M.; Du Prez, F. E. Vitrimers: permanent organic networks with glass-like fluidity. *Chem. Sci.* **2016**, *7*, 30–38.
- (44) Xiang, H. P.; Rong, M. Z.; Zhang, M. Q. A facile method for imparting sunlight driven catalyst-free self-healability and recyclability to commercial silicone elastomer. *Polymer* **2017**, *108*, 339–347.
- (45) Xiang, H.; Yin, J.; Lin, G.; Liu, X.; Rong, M.; Zhang, M. Photocrosslinkable, self-healable and reprocessable rubbers. *Chem. Eng. J.* **2019**, *358*, 878–890.
- (46) Amamoto, Y.; Otsuka, H.; Takahara, A.; Matyjaszewski, K. Self-healing of covalently cross-linked polymers by reshuffling thiuram disulfide moieties in air under visible light. *Adv. Mater.* **2012**, *24*, 3975–3980.
- (47) Zhao, D.; Du, Z.; Liu, S.; Wu, Y.; Guan, T.; Sun, Q.; Sun, N.; Ren, B. UV light curable self-healing superamphiphobic coatings by photopromoted disulfide exchange reaction. *ACS Appl. Polym. Mater.* **2019**, *1*, 2951–2960.
- (48) Otsuka, H.; Nagano, S.; Kobashi, Y.; Maeda, T.; Takahara, A. A dynamic covalent polymer driven by disulfide metathesis under photoirradiation. *Chem. Commun.* **2010**, *46*, 1150–1152.
- (49) Michal, B. T.; Jaye, C. A.; Spencer, E. J.; Rowan, S. J. Inherently photohealable and thermal shape-memory polydisulfide networks. *ACS Macro Lett.* **2013**, *2*, 694–699.
- (50) Santana, M. H.; Huete, M.; Lameda, P.; Araujo, J.; Verdejo, R.; López-Manchado, M. A. Design of a new generation of sustainable SBR compounds with good trade-off between mechanical properties and self-healing ability. *Eur. Polym. J.* **2018**, *106*, 273–283.
- (51) Takahashi, A.; Goseki, R.; Otsuka, H. Thermally Adjustable Dynamic Disulfide Linkages Mediated by Highly Air-Stable 2, 2, 6, 6-Tetramethylpiperidine-1-sulfonyl (TEMPS) Radicals. *Angew. Chem., Int. Ed.* **2017**, *56*, 2016–2021.
- (52) Takahashi, A.; Goseki, R.; Ito, K.; Otsuka, H. Thermally healable and reprocessable bis (hindered amino) disulfide-cross-linked polymethacrylate networks. *ACS Macro Lett.* **2017**, *6*, 1280–1284.
- (53) Hu, Y.; Tang, G.; Luo, Y.; Chi, S.; Li, X. Glycidyl azide polymer-based polyurethane vitrimers with disulfide chain extenders. *Polym. Chem.* **2021**, *12*, 4072–4082.
- (54) Eidi, M.; Pedram, M. Z. Thermal induced intrinsic self-healing in epoxy based elastomer coatings provided by disulfide metathesis reactions. *J. Appl. Polym. Sci.* **2022**, *139*, No. 52239.
- (55) Wu, X.; Li, J.; Li, G.; Ling, L.; Zhang, G.; Sun, R.; Wong, C. P. Heat-triggered poly (siloxane-urethane) s based on disulfide bonds for self-healing application. *J. Appl. Polym. Sci.* **2018**, *135*, No. 46532.
- (56) Xiang, H. P.; Qian, H.; Lu, Z.; Rong, M.; Zhang, M. Crack healing and reclaiming of vulcanized rubber by triggering the rearrangement of inherent sulfur crosslinked networks. *Green Chem.* **2015**, *17*, 4315–4325.
- (57) Lei, Z. Q.; Xiang, H. P.; Yuan, Y. J.; Rong, M. Z.; Zhang, M. Q. Room-temperature self-healable and remoldable cross-linked polymer based on the dynamic exchange of disulfide bonds. *Chem. Mater.* **2014**, *26*, 2038–2046.
- (58) Deliballi, Z.; Demir-Cakan, R.; Kiskan, B.; Yagci, Y. Self-Healable and Recyclable Sulfur Rich Poly (vinyl chloride) by S–S Dynamic Bonding. *Macromol. Chem. Phys.* **2022**, No. 2100423.
- (59) Deng, G.; Li, F.; Yu, H.; Liu, F.; Liu, C.; Sun, W.; Jiang, H.; Chen, Y. Dynamic hydrogels with an environmental adaptive self-healing ability and dual responsive sol–gel transitions. *ACS Macro Lett.* **2012**, *1*, 275–279.
- (60) Hernández, M.; Grande, A. M.; Dierkes, W.; Bijleveld, J.; Van Der Zwaag, S.; García, S. J. Turning vulcanized natural rubber into a self-healing polymer: Effect of the disulfide/polysulfide ratio. *ACS Sustainable Chem. Eng.* **2016**, *4*, 5776–5784.
- (61) Martin, R.; Rekondo, A.; De Luzuriaga, A. R.; Casuso, P.; Dupin, D.; Cabañero, G.; Grande, H. J.; Odriozola, I. Dynamic sulfur chemistry as a key tool in the design of self-healing polymers. *Smart Mater. Struct.* **2016**, *25*, No. 084017.
- (62) Shao, C.; Chang, H.; Wang, M.; Xu, F.; Yang, J. High-strength, tough, and self-healing nanocomposite physical hydrogels based on the synergistic effects of dynamic hydrogen bond and dual coordination bonds. *ACS Appl. Mater. Interfaces* **2017**, *9*, 28305–28318.
- (63) Lafont, U.; Van Zeijl, H.; Van Der Zwaag, S. Influence of cross-linkers on the cohesive and adhesive self-healing ability of polysulfide-based thermosets. *ACS Appl. Mater. Interfaces* **2012**, *4*, 6280–6288.
- (64) Parker, R.-E.; Isaacs, N. Mechanisms of epoxide reactions. *Chem. Rev.* **1959**, *59*, 737–799.
- (65) Ehlers, J.-E.; Rondan, N. G.; Huynh, L. K.; Pham, H.; Marks, M.; Truong, T. N. Theoretical study on mechanisms of the epoxy–amine curing reaction. *Macromolecules* **2007**, *40*, 4370–4377.
- (66) Nevejans, S.; Ballard, N.; Miranda, J. I.; Reck, B.; Asua, J. M. The underlying mechanisms for self-healing of poly (disulfide) s. *Phys. Chem. Chem. Phys.* **2016**, *18*, 27577–27583.
- (67) Azcune, I.; Odriozola, I. Aromatic disulfide crosslinks in polymer systems: Self-healing, reprocessability, recyclability and more. *Eur. Polym. J.* **2016**, *84*, 147–160.
- (68) de Luzuriaga, A. R.; Martin, R.; Markaide, N.; Rekondo, A.; Cabañero, G.; Rodríguez, J.; Odriozola, I. Epoxy resin with exchangeable disulfide crosslinks to obtain reprocessable, repairable and recyclable fiber-reinforced thermoset composites. *Mater. Horiz.* **2016**, *3*, 241–247.
- (69) Richards, R. B. Polyethylene-structure, crystallinity and properties. *J. Appl. Chem.* **2007**, *1*, 370–376.
- (70) Eom, Y.; Kim, S.-M.; Lee, M.; Jeon, H.; Park, J.; Lee, E. S.; Hwang, S. Y.; Park, J.; Oh, D. X. Mechano-responsive hydrogen-bonding array of thermoplastic polyurethane elastomer captures both strength and self-healing. *Nat. Commun.* **2021**, *12*, No. 621.